Chalcogenide Letters Vol. 13, No. 8, August 2016, p. 339 - 350

EFFECT OF THE pH ON CRYSTAL STRUCTURAL, OPTICAL AND SURFACE MORPHOLOGICAL PROPERTIES OF THE CdS FILMS DEPOSITED BY CHEMICAL BATH DEPOSITION

A. S. AYBEK[a*], H. RÜZGAR[b]
[a]*Department of Physics, Anadolu University, Eskisehir 26470, Turkey*
[b]*Graduate School of Sciences, Anadolu University, Eskisehir 26470, Turkey*

Cadmium sulphide films have been deposited from aqueous solutions onto the glass substrates by chemical bath deposition method at different pH values (10.30, 10.35, 10.40, 10.45 and 10.50) at 80 ^{o}C. The crystal structure and the size of the crystallites in the film were characterized from X-ray diffraction patterns. XRD pattern of the films showed cubic phase with preferred (111) orientation and the grain sizes were calculated between 31-107 nm. The thicknesses of the CdS films were determined to be between 85-200 nm. The band gap of the films was obtained from the absorbance measurements in the visible range. The optical absorption studies reveal that the transition is direct with band gap energy values between 2.33 and 2.39 eV. The transmission efficiency of CdS films were exhibit about between 50%-65% in the visible region. The surface morphology of the films was characterized by atomic force microscopy and field emission scanning electron microscope. The deep energy level is estimated about 0.6 eV below the conduction band.

(Received June 28, 2016; Accepted August 4, 2016)

Keywords: CdS, Chemical bath deposition, pH effect, Structural and optical properties, Deep trap

1. Introduction

Cadmium sulphide (CdS) is one of the most important II-VI compound semiconductor materials with a wide and direct band gap of 2.32-2.45 eV [1-3]. CdS material shows n-type semiconduction properties because of sulphur defiency [4]. CdS can grow with different crystal structures such as f.c.c. (zinc blende), h.c.p. (wurtzite) and mixed structure depending on deposition conditions [4-6]. Bulk crystalline CdS crystallize in the wurtzite form, while in nano-scale the cubic form is the predominant [4]. CdS thin film has been used various applications such as solar cells [7], thin film transistors [5], light-emitting diodes [8]. It has also CdS films have been widely used as n-type semiconducting partners or buffer layers for high-efficiency Cu(In,Ga)Se_2[5,7], PbS [1], Cu_2S [9] or CdTe solar cells [10,11]. The quality of the CdS plays an important role for solar cell applications, CdS films need to have a suitable conductivity, and adequate thickness to allow high transmission [12]. CdS films can be deposited using several techniques such as successive ionic layer adsorption and reaction (SILAR) [13], vacuum evaporation (VE) [10], close-spaced sublimation (CSS) [11], RF sputtering [11], spray pyrolysis [14], electro-chemical deposition (ECD) [4], and chemical bath deposition (CBD) [5,11]. Among these various methods, the CBD is considered as the best method to obtain large-area at low cost and low temperature CdS thin films for photovoltaic device applications [5,15-17]. It is possible to produce uniform films with good adherence reproducibly by CBD [3]. In CBD method, the structure of the films is influenced by the deposition parameters such as composition of the bath, temperature, deposition time, pH of the solution [18]. CBD-CdS films give excellent results for solar cell applications because of their relatively high photoconductivity and morphological

*Corresponding author: saybek@anadolu.edu.tr

properties [19]. In literature abundant research reports are available about CdS, but rarely any report available on use of pH effect for improving the properties in CdS films [20].

In this work, the CdS films deposited by the CBD method are suitable for scientific studies and technological applications. The present investigation has two purposes: (i) deposited of a film onto glass substrates with different pH values (ii) the effect of aqueous solution pH, in order to improve the film properties. The effects of pH on crystal structural, optical and morphological properties of the CdS films have been investigated in order to study the film deposited mechanism.

2. Experimental Details

2.1. Preparation of CdS films

In this present work, the CdS films were deposited onto pre-cleaned glass microscope substrates by CBD method at 80˚C bath temperature. The glasses (13 x 75 x 1.0 mm^3) were used as substrates boiled in detergent solution, and then rinsed with distilled water and dried by compressed air. The dried glass substrates were cleaned ultrasonically by distilled water for about 15 min and dried again under compressed air. Finally, they were etched in acetone and propane at room temperature, dried by compressed air.

Aqueous solutions of 0.02 M $CdCl_2 \cdot H_2O$, 0.5 M KOH, 1.5 M NH_4NO_3 and 0.2 M thiourea (H_2NCSNH_2) were chosen as a precursor for the preparation of the CdS films. The films were deposited using cadmium chloride precursor as Cd source and thiourea as S source respectively. The addition of ammonia solution slowly dropped into the bath solution to adjust the pH to10.30, 10.35, 10.40, 10.45 and 10.50, respectively. The CdS films were deposited onto glass substrates labelled to easy understand A, B, C, D and E with pH= 10.30, 10.35, 10.40, 10.45 and 10.50, respectively. The chemical bath solutions were continuously stirred to obtain a homogeneous mixture. The bath solution is clear and transparent at the beginning of the reaction. The colour of the solution changed during the deposition from light yellow to orange. The reaction of the CdS formation on the substrates can be given as:

$$CdCl_2 + 2KOH \longrightarrow Cd(OH)_2 + 2KCl, \quad (1)$$

$$Cd(OH)_2 + 3NH_4NO_3 \longrightarrow [Cd(NH_3)_4](NO_3)_2 + 2O_2 + H_2O \quad (2)$$

$$[Cd(NH_3)_4)](NO_3)_2 \longrightarrow Cd(NH_3)_4^{2+} + 2NO_3^- \quad (3)$$

$$Cd(NH_3)_4^{2+} \longrightarrow Cd^{2+} + 4NH_3 \quad (4)$$

$$CS(NH_2)_2 + 2H_2O \longrightarrow 2NH_3 + CO_2 + H_2S \quad (5)$$

$$H_2S \longrightarrow S^{2-} + 2H^+, \quad (6)$$

$$Cd_{eq}^{2+} + S_{eq}^{2-} \longrightarrow CdS \quad (7)$$

The glass substrates were placed vertically inside the glass beaker and the deposition in the bath was carried out at 80˚C for 40 minutes. After the deposition process, the produced CdS films were washed softly in distilled water to remove some unwanted and loose particles on their surface, and dried in air at 80˚C temperature in oven. The deposited CdS films were seen homogenous, well adherent to the glass substrates and having a shiny. The growths of films were seen better front side of the glasses. The films on back side of the substrate were removed by using nitric acid, while on the other side were used for all the measurements.

The average thickness of all the CdS films was determined by using TT-90 Spectroscopic Ellipsometer. The thicknesses of the films were obtained between 85-200 nm and these values are given in Table 2.

The C film deposited onto fluorine doped tin oxide (FTO) conducting substrate by CBD method for electrical measurement. The sandwich structure of the metal–semiconductor–metal system has been obtained by vacuum deposition of the gold electrodes on the film as top electrode by using Leybold Heraus 300 Univex System. The space between the electrodes was 200 nm that it is the thickness of C film and the area of the top electrode was about 2 mm^2. Copper wires were attached to the top and bottom electrodes by small droplets of silver paste. The electrical measurement was carried out in dark medium by using Agilent 34401Model Digital Multimeter,

HP 4140B pA meter/dc voltage source, and VEE One Lab 6.1 Computer Program. The sample was kept it in dark for 30 min before measurement. The C film is electrically conductive n-type semiconductor as determined from the hot probe method.

2.2. Characterization of CdS films

Characterizations of the CdS films were performed at room temperature. The crystal structural analyses of all the films were determined by Bruker D8-X-Ray Diffractometer. The diffraction angle 2θ was set between 20^o and 65^o using CuK_α (λ=1.5406 Å) radiation with scan rate 0.1 sec/step.

The optical absorbance and transmittance data of the films were carried out using SolidSpec-3700 UV-VIS-NIR Spectrophotometer in the wavelength range from 350 to 1000 nm.

Surface morphology of the films was characterized using ScanAtomic SPM software-2009 (AFM) and Zeiss Ultra Plus Field Emission Scanning Electron Microscope (FESEM).

3. Result and Discussion

3.1. Crystal structural properties of the CdS films

The crystal structure and orientation of the CdS films were investigated by XRD patterns. Figure 1 shows the diffraction patterns of all the films deposited at different pH values of the bath solutions. The main existence of diffraction peak at 2θ position about 26.7^o CdS from ICDD (International Centre for Diffraction Data) card no 01-089-0440 in A and B are crystallized in the face-centred cubic phase. 2θ position about27.1^o α-CdS, Hawleyite from ICDD: 03-065-8873 in C, D and E. According to the Fig. 1, the films have (111) as the preferred orientation. It is observed that the highest peak (111) reflection in the XRD patterns is observed at C. The highest peak in the XRD pattern means that the crystallization was good. Thus, the pH control in the growth solutions produces CdS films with higher crystallinity [21]. We may say that this diffraction patterns shows that the films are single crystalline character [6]. Another reflection peak (220) and (311) are also seen with comparatively lower intensities.

The intensity of the observed peaks in the XRD pattern for the CdS films, we fit the XRD peaks into Gaussian to determined Bragg angle (in Table 1.) and full width at half maximum (*FWHM*) of the peaks. The XRD patterns of CdS are found to be best fitted to Gaussian peak by using computer program (in Fig.1. inset). The program uses a Marquardt–Levenberg algorithm to minimize the difference between the experimental data and the fitting equation.

It is seen that the peak intensity and Bragg angle change with the values of pH of the bath solution in the XRD patterns. It can be concluded that the pH of in the bath affects the formation of CdS films. The XRD measurements were performed to follow the change of crystallinity induced by the pH effect of the chemical bath solution. XRD patterns indicated that with changing pH value of the solution and the CdS film structure changes from CdS (FCC) to α-CdS (Hawleyite). CdS film structure transforms from cubic structure to mixed cubic and hexagonal structure by increasing the pH values of the bath solution reported in the literature [22]. In the literature nano-scale crystalline CdS crystallize in the cubic forms is the predominant [4]. Therefore, we can say that the crystal structures of CdS films are face-centred cubic and Hawleyite phase, the thicknesses of films within the range 85 nm to 200 nm.

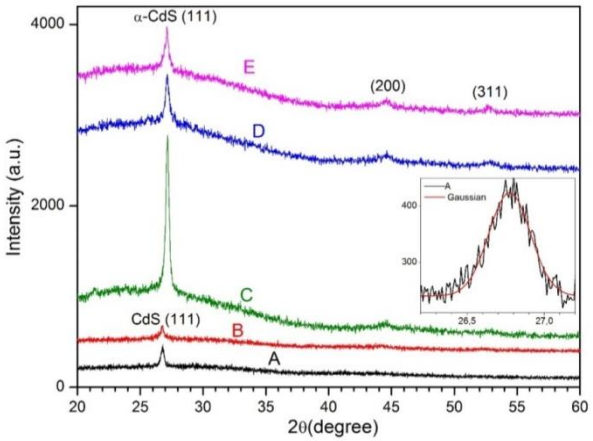

Fig. 1. XRD patterns of the CdS films deposited by the CBD method with different pH solutions, (A, B, C, D and E).

It is possible the change of the lattice parameter when the crystal structure of the CdS films changes from CdS to α-CdS. The lattice parameters for cubic CdS films has been evaluated using following relation given by [23]

$$\frac{1}{d^2} = \frac{(h^2+k^2+\ell^2)}{a^2} \tag{8}$$

where d is the interplanar distance, ($hk\ell$) are Miller indices of the lattice plane, a is the lattice parameters of the crystal structure of the CdS films. The calculated and standard, lattice parameters and interplanar distance are given in the Table 1.

Table 1. Lattice constant value of the CdS films with different pH solutions.

pH		2 θ (degree)	d (Å)		(h k ℓ)	a (Å)	
			calculated	standard		calculated	standard
A	CdS	26.748	3.323	3.330	(111)	5.757	5.830
B		26.799	3.323			5.757	
C	α-CdS	27.181	3.278	3.303		5.677	5.720
D		27.142	3.282			5.685	
E		27.122	3.285			5.689	

As seen in the Table 1., the lattice parameters values of all the films for preferred orientation along (111) planes are smaller than those of the corresponding standard material for CdS and α-CdS films. The CdS films structure changes from CdS to α-CdS structure. This situation is causing strain in the crystal structure. Between calculated and standard of the lattice parameter values difference could be attributed to the strain introduced in the films due to excess Cd interstitials or S vacancies present in the films. As seen in Table 1., defects such as strain has the smaller value for the films at α-CdS than at CdS, which may be due to the improvement in the crystallinity and stoichiometry of the film deposited at that pH's as evident from XRD patterns (this point will be considered later in this section) [14].

The strain in the CdS films have been determined using the equation

$$\beta = \frac{\lambda}{D\cos\theta} - \varepsilon \tan\theta \tag{9}$$

where β is the *FWHM* determined from Gaussian fit, λ the wavelength, θ the Bragg angle, D the grain size and ε the strain. β cosθ/λ versus sinθ/λ plots for the CdS films are shown in Fig. 2. The

slopes of the graphs give the values of average strain (ε) in the films. From the XRD pattern of the CdS films, it can be seen that the diffraction peaks a slight shift regarding their normal position. This is due to the deformation in the films and is called macro strain. The macro strains in the films have reached the maximum value in C as seen in Table 2. [24].

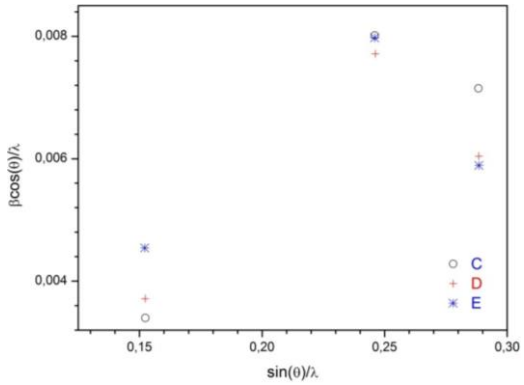

Fig. 2. $\beta\ cos(\Theta)/\lambda$ vs. $sin\ (\Theta)/\lambda$ plots for the CdS films.

Table 2. Microstructural parameter of the CdS films with different pH solutions.

CdS	Thickness (nm)	Strain ε	D (nm)	Dislocation density γx10^{13}(lines/m^2)
A	130	....	31	104
B	85	....	37	73
C	200	0.0312	105	9.07
D	135	0.0214	107	8.73
E	166	0.0143	35	82

The grain sizes of the CdS films are estimated from the extrapolation of the graph to sin θ = 0 gives 1/D as the intercept on the $\beta\ \cos(\Theta)/\lambda$ axis. The grain size values of the CdS films were given in Table 2. It is also observed that the grain sizes values changed of the films with the increase of pH values of the bath.

XRD patterns of the A and B have got only one peak, therefore the grain sizes of these films were estimated using by Debye-Scherrer's formula [22].

$$D = \frac{0.9\lambda}{\beta cos\theta} \tag{10}$$

β values for the CdS films peak have been calculated using the fit and the average crystallite sizes have been estimated by Debye-Scherrer's formula [21]. The crystallite sizes for A and B films are given in Table 2. This may indicate that ion by ion deposition dominated the deposition process and as a result a much smaller grain size and thinner films were obtained. Similar grain size values of CdS films by deposited CBD have been reported by literature [9,25]. The grain size of the films changed with increasing pH.

The dislocation density (γ) defined as the length of dislocation lines per unit volume of the crystal has been deduced from this formula;

$$\gamma = \frac{C}{D^2} \tag{11}$$

where c is taken as unity at minimum dislocation density. The variation of dislocation density as a function of pH solution is shown in Fig. 3. It is observed that the dislocation density reaches the minimum values for C and D films in Fig. 3. This is proof that these films crystalline defects are

less than in the other films. The decrease in dislocation density indicates the decrease in the concentration of lattice imperfections, and better crystallization of films [26].

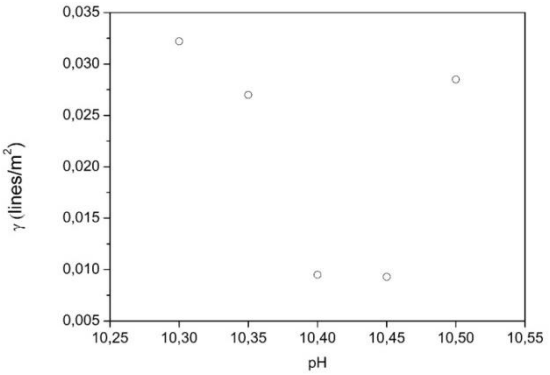

Fig. 3. Variation of dislocation density as a function of pH solution for the CdS films.

3.2. Optical properties of the CdS films

The optical absorbance spectra of the CdS films by the CBD method with different pH solution are shown in Fig. 4.

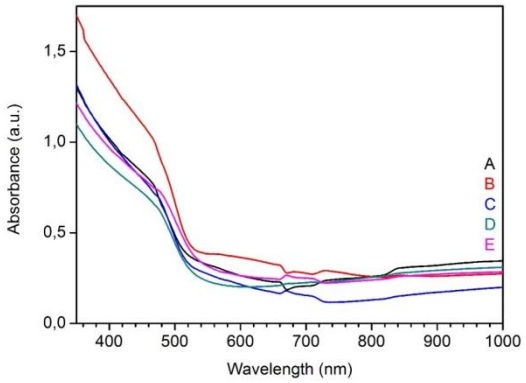

Fig. 4. Optical absorbance spectra of the CdS films deposited with different pH solution.

It is shown that a sharp rise in absorbance occurs between 500 and 550 nm. These regions are called fundamental absorption edges. The fundamental absorption refers to band to band transition, i.e., to the excitation of an electron from the valance band to the conduction band. The fundamental absorption can be used to determine the energy gap of the semiconductor films. The optical band gap E_g is deduced from the formula [27],

$$\alpha h\nu \approx (h\nu - E_g)^n \tag{12}$$

where α is the absorption coefficient, h is the Planck's constant, ν is the photon frequency, E_g is the optical band gap of the CdS films and n is equal to 1/2 for direct band transition gap material such as CdS [28]. The absorption coefficient being about 10^4 cm^{-1}, which is deduced from the absorption spectra, is also an indication of the direct transition. The optical band gap of the CdS films were calculated by plotting $(\alpha h\nu)^2$ versus $h\nu$. They were determined from the intercept of the straight-line portion of the $(\alpha h\nu)^2$ versus $h\nu$graph on the $h\nu$ axis. It is seen that the band gap energy values as shown in the Fig. 5. (A-E).

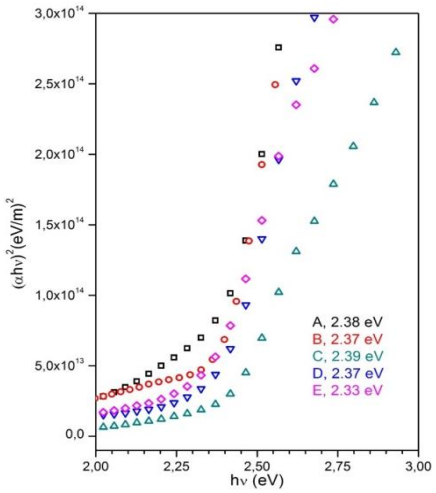

Fig. 5. Energy gaps of the CdS films deposited with different pH solution.

In this work we obtained CdS films deposited by CBD with band gap values that vary from 2.33 eV to 2.39 eV. As It can be seen that the calculated direct band gap values are shown in Table 3. It is indicated that the CdS film band gap values changed a few with varying pH. The band gap values are in good agreement with previously reported values for CdS films produced by chemical bath deposition [2,5,11,17].

Table 3. Energy gaps of the CdS films deposited with different pH solution.

Films	E_g(eV)
A	2.38
B	2.37
C	2.39
D	2.37
E	2.33
Reported	2.38[2]
	2.34[5]
	2.39[11]
	2.41, 2.42[17]

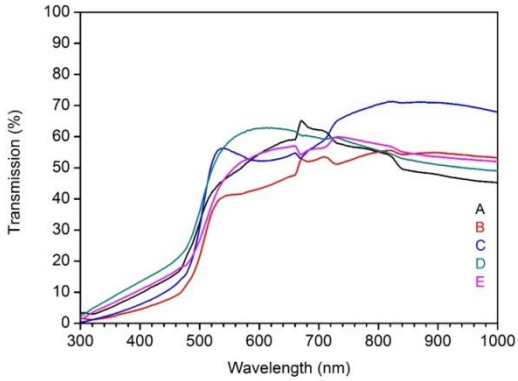

Fig. 6. Optical transmittance spectra of the CdS films deposited with different pH solution.

Fig. 6. shows the optical transmission spectra of the CdS films deposited by the CBD method with different pH values. All films have a sharp absorption edge near 500 nm, which

corresponds to the energy band gap of films. The films exhibited transparency in the visible region. It can be seen that the average transmission values are 60% in the wavelength range after 500 nm.

Absorption of light in the longer wavelength region ($\lambda \geq 510$ nm) is usually caused by crystalline defects such as grain boundaries and dislocations that are responsible of the reduction in the optical transmission [17, 29]. This indicates that varying pH introduces a large amount of defects into CdS films (especially A, B and E), which agrees with dislocation density values in Table 3.

3.3. Morphological properties of the CdS films

3-D (4 μm × 4 μm) AFM images of CdS films are shown in Fig. 7. (a-e). According to the images, which presents grains with sphere shape and different sizes greater than 20 nm. A quantitative way to study the quality of the CdS film surface morphology is presented the root mean square (rms) roughness and the average roughness value measured on the film surface. The surface rms roughness and the average roughness values determined from using surface roughness measurements from AFM images are shown in the Table 4. It can be seen that the roughness values of the C and D films are smaller value than the others in Table 4. The small roughness value indicates that surface of the film smooth, uniform and dense. We can say that surface of the C and D films are smooth. Also, due to the small dislocation density exhibits which the film is a proof that surface of the film is smooth. Thus the surface roughness of the films changes with different pH values and as a result both the strain and dislocation density changes.

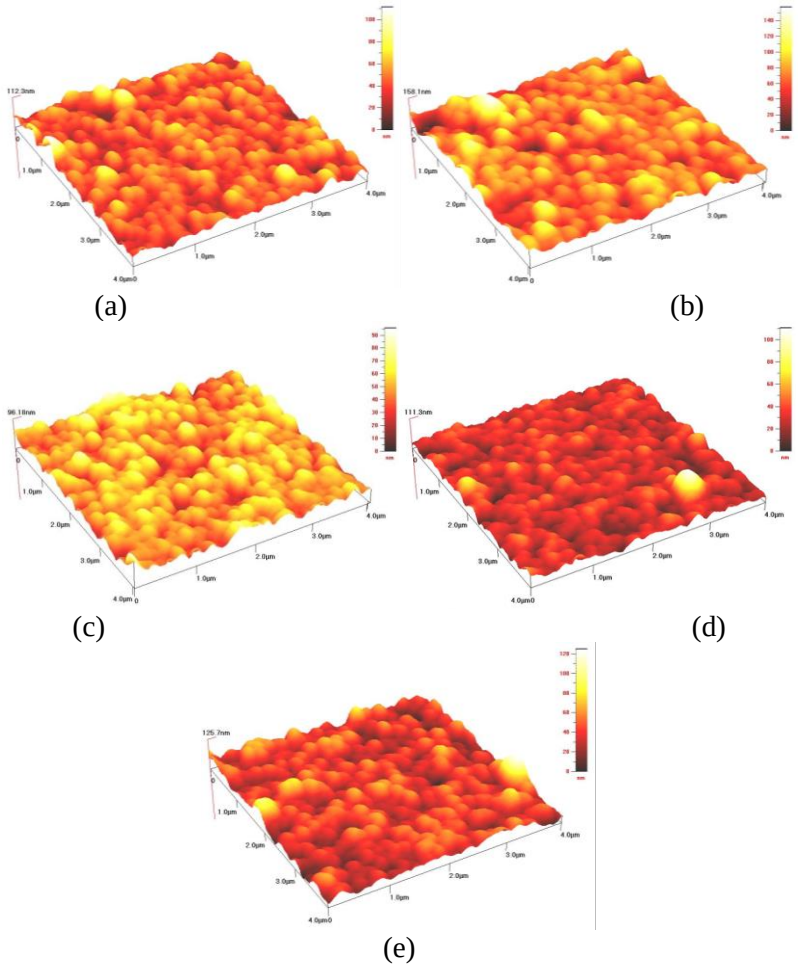

Fig. 7. AFM images of the CdS films deposited by the CBD method with different pH solution (a) A, (b) B, (c) C, (d) D, (e) E.

Table 4.Surface rms roughness and average roughness values of the CdS films.

CdS Films	A	B	C	D	E
rms roughness(nm)	11.5	15.7	9.36	10.5	12.5
average roughness(nm)	8.92	11.9	7.54	8.15	10.0

Fig. 8. (a-e) shows FESEM images of the CdS film at 100,000 magnifications with different pH values. It is seen that the surface morphologies of CdS films are dense and homogeneous. The substrates are well covered by many small cubic crystalline grains confirming the fact that the deposited mechanism takes place of ion-by-ion mechanism [14].The CdS films do not show any void, pinholes or cracks, except for the one deposited at E. It can be seen that the morphology is not smooth, a few cracks appear. The films are composed of regular grains with approximately 100 nm diameters and no pinholes were found at C and D. This result is compatible with the grain sizes estimated from XRD patterns of the films. The FESEM images show different morphologies of the surface grains, which may be due to different pH values. Our results show that the pH effect of CdS films has positive effects to improve the film quality as the window layer for solar cell applications. These results are also supported by the FESEM images, the small values of the dislocation densities and roughness.

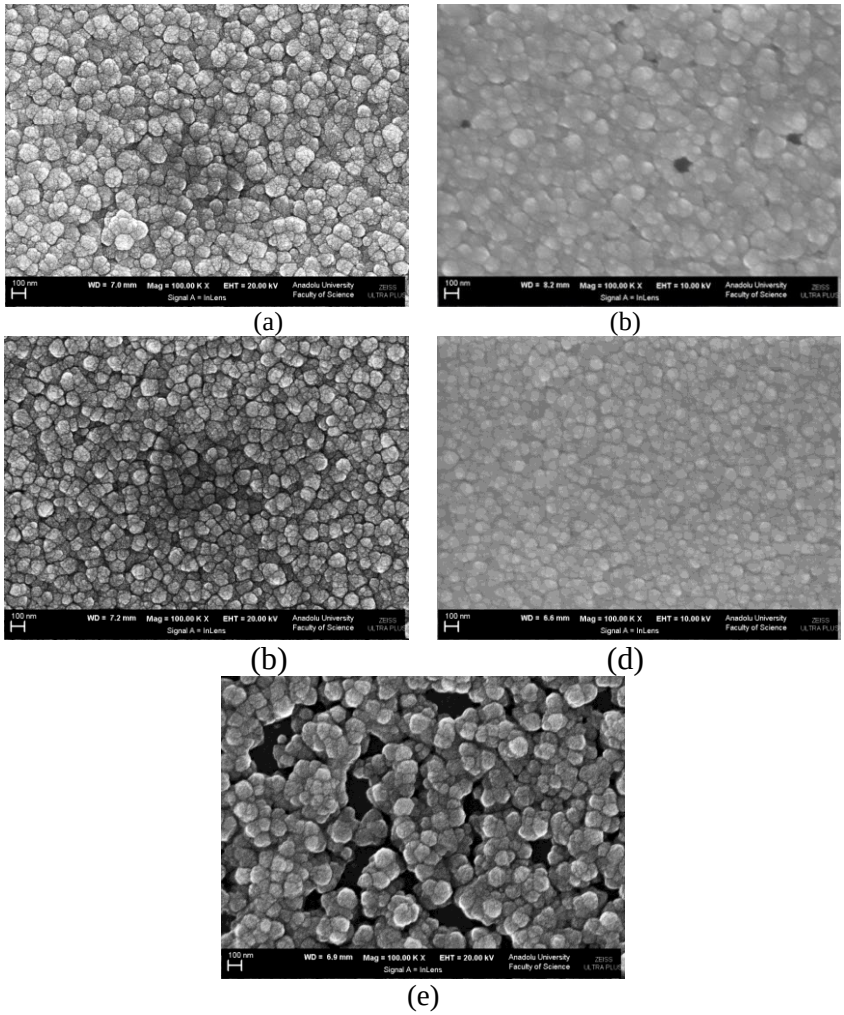

Fig. 8. FESEM images of the CdS films deposited by the CBD method in different pH solution (a) A, (b) B, (c) C, (d) D, (e) E.

3.4. Electrical properties of the CdS film at pH 10.40

The crystal structure of the film plays an important role in the electrical properties of semiconductor films. The electrical properties of the semiconductor films have been determined from the *I*-*V* characteristics. In Fig. 9., the current-voltage characteristics of the sandwich structure of the metal-semiconductor-metal samples were found to be of the form $I \sim V^m$ where *I* is current, *V* is the applied voltage, and *m* is the slope of the log *I* versus log *V* curve. We see that there are three conduction regions: Ohmic region at low voltages where *I* is proportional to *V* with m≈1, trap-filled-limited current (TFL) region where the current rises sharply, in fact nearly vertically, with voltage $V \approx V_{TFL}$, and trap free region where *I* is proportional to *V* with m is greater than 1.

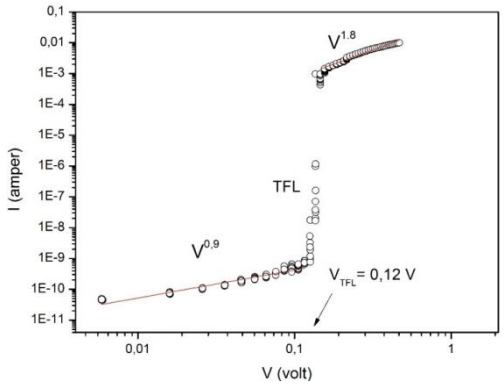

Fig. 9. The current-voltage characteristic of the CdS film.

In the presence of the effect of the traps that is given by the current-voltage relation

$$J = \frac{9}{8}\frac{\varepsilon_o \varepsilon_r \mu \theta_o V^2}{t^3} \tag{13}$$

where ε_o is the permittivity of free space, ε_r the relative permittivity of semiconductors [30], μ the free carriers mobility, t the separation between the electrodes, θ_o is the ratio of free-to-trapped charge, it is indeed equal to one for the trap-free case. θ_o is given by

$$\theta_o = \frac{N_C}{N_T} e^{-\frac{E_T}{kT}} \tag{14}$$

here N_C is effective density of states in conduction band (1.10^{26} m^{-3}) of semiconductor, N_T the number of traps per unit value at energy E_T from the bottom of conduction band, and kT thermal energy (≈0.025 eV at room temperature) of charge carrier.

Another point of interest in Fig. 9. is that at voltage $V=V_{TFL}$ which is trap-filled-limited voltage, all the traps will become full and the current will rise rapidly by an θ_o^{-1} amount. This voltage is given as

$$V_{TFL} = \frac{eN_T t^2}{2\varepsilon_o \varepsilon_r} \tag{15}$$

where *e* is the electron charge. The space-charge-limited conduction is a fruitful mechanism in a way that one can get an idea about some of parameters of the materials such as density and trap energy level, and if the crossover is directly from Ohm's law to the *TFL* regime in the current-voltage characteristics, the semiconductor has deep trap energy level [31]. The determined values of parameters are given in Table 5.

Table 5.Some of the parameters of the CdS film at pH 10.40 being investigated.

	θ_o	$N_T(m^{-3})$	E_T(eV)
C film	$7{,}1410^{-6}$	$1{,}56x10^{21}$	0,57

Examining Table 5., we see that the deep trap energy level is estimated about 0.6 eV below the conduction band in the energy gap. In literature, for E_T values it could be evaluated as $E_T < 0.1$ due to the chemisorbed oxygen atoms at the film surface and the heavy concentration of carriers and the presence of adsorbed oxygen at the grain boundaries, and $E_T > 0.1$ due to the defects at localized states [32] that they are attributed to the recombination of charge carriers [33-35], and sulphur vacancies etc. [36,37].

4. Conclusions

CdS films have been deposited onto the glass substrates by the CBD method at 80 ^oC bath temperature. The effects of pH on the crystal structural, optical and morphological properties of CdS films were investigated. X-ray diffraction studies revealed that the deposited CdS films structure changes from cubic to α-cubic crystal structure by increasing the pH values of the bath solution. The grain size of CdS films were found to be between 31-107 nm. pH values effect can obviously promote the crystal structure of CdS films, especially at pH 10.40. The optical band gap energy values of the films varied from 2.33 to 2.39 eV. The AFM and FESEM micrographs showed that the surface morphology is affected by the pH. The pH causes a decrease in the rms roughness, which provided that surface smoothness especially at pH 10.40. In conclusion, well crystallized, low values roughness parameters, the transmittance (~60%) and wide band gap (2.39 eV) obtained for the films deposited at pH 10.40. It is also determined that deep trap energy level from the electrical result for pH 10.40 CdS film. Consequently, we can say that different pH value of solution affects the crystalline structural, optical and morphological of CdS films.

Acknowledgments

This work have been supported by Anadolu University (Project Number: 1307F291), authors thank the Faculty of Science Anadolu University for XRD measurements.

References

[1] A.S. Obaid, Z. Hassan, M.A. Mahdi, M. Bououdina, Sol. Energy **89**, 143 (2013).
[2] M.A. Islam, M.S. Hossain, M.M. Aliyu, P. Chelvanathan, Q. Huda, M.R. Karim, K. Sopian, N. Amin, Energy Procedia **33**, 203 (2013).
[3] L. Kong, J.Li, G. Chen, C. Zhu, W.Liu, J. Alloy Compd. **573**, 112 (2013).
[4] A. Zyoud, I. Saa'deddin, S. Khudruj, Z.M. Hawash, D. Park, G. Campet, H.S. Hilal, Solid State Sci. **18**, 83 (2013).
[5] J.-H. Kwon, J.-S. Ahn, H. Yang, Curr. Appl. Phys. **13**, 84 (2013).
[6] E. Yücel, N. Güler, Y. Yücel, J. Alloy Compd. **589**, 207 (2014).
[7] R.N. Bhattacharya, K. Ramanathan, Sol. Energy **77**, 679 (2004).
[8] J. Zhao, J.A. Bardecker, A.M. Munro, M.S. Liu, Y. Niu, I-K. Ding, J. Luo, B. Chen, A. K.-Y. Jen, D.S. Ginger, Nano Lett. **6**, 463 (2006).
[9] V.S. Taur,R.A. Joshi,A.V. Ghule, R. Sharma, Renew. Energ. **38**, 219 (2012).
[10] J. Lee, Appl. Surf. Sci. **252**, 1398 (2005).
[11] G. Pérez-Hernández, J. Pantoja-Enríquez, B. Escobar-Morales, D. Martinez-Hernández, L.L. Díaz-Flores, C. Ricardez-Jiménez, N.R. Mathews, X. Mathew, Thin Solid Films **535**, 154 (2013).

[12] D. Kim, Y. Park, M. Kim, Y. Choi, Y.S.Park, J. Lee, Mater. Res. Bull. **69**, 78 (2015).
[13] M. Kundakci, A. Ateş, A. Astam, M. Yildirim, Physica E **40**, 600 (2008).
[14] T.Sivaraman, V.S. Nagarethinam, A.R.Balu, Res. J. Material Sci. **2**(2), 5 (2014).
[15] J.N. Ximello-Quiebras, G. Contreras-Puente, G. Rueda-Morales, O. Vigil, G. Santana-Rodríguez, A. Morales-Acevedo, Sol. Energ. Mat. Sol. C. **90**, 727 (2006).
[16] I.O. Oladeji, L. Chow, Thin Solid Films **474**, 77 (2005).
[17] F. de Moure-Flores, K.E. Nieto-Zepeda, A. Guillén-Cervantes, S. Gallardo, J.G. Quiñones-Galván, A. Hernández-Hernández, M. de la L. Olvera, M. Zapata-Torres, YuKundriavtsev, M. Meléndez-Lira, J. Phys. Chem. Solids **74**, 611 (2013).
[18] J.P. Enríquez, X. Mathew, Sol. Energ. Mat. Sol. C.76, 313–322 (2003).
[19] M. Estela Calixto, M. Tufiño-Velázquez, G. Contreras-Puente, O. Vigil-Galán, M. Jiménez-Escamilla, R. Mendoza-Perez, J. Sastré-Hernández, A. Morales-Acevedo, Thin Solid Films **516**, 7004 (2008).
[20] J. Li, Preparation and properties of CdS thin films deposited by chemical bath deposition, Ceram. Int.**41**, S376 (2015).
[21] R. Ochoa-Landín, M.G.Sandoval-Paz, M.B.Ortun˜o-Lo´ pez, M.Sotelo-Lerma, R.Ramı´rez-Bon, J. Phys. Chem. Solids **70**, 1034 (2009).
[22] H. Zhan, J. kang Li, Y. fei Cheng, Optik **126**, 1411 (2015).
[23] B.D. Cullity, Elements of X-Ray Diffraction, edited by M. Cohen, Addison-Wesley, Publishing Company (1956).
[24] F.C. Eze, Mater. Chem. Phys. **89**, 205 (2005).
[25] H. Metin and R. Esen, Semicond. Sci. Technol. **18**, 647 (2003).
[26] K. Mageshwari, R. Sathyamoorthy, Mat. Sci. Semicon. Proc. **16**, 337 (2013).
[27] J.I. Pankove, Optical Processes in Semiconductors, Prentice-Hall, Engle wood Cliffs, NJ (1971).
[28] H. Khallaf, I.O. Oladeji, G. Chai, L. Chow, Thin Solid Films **516**, 7306 (2008).
[29] J.Y. Choi, K.-J. Kım, J.-B. Yooand D. Kım, Sol. Energy **64**(1), 341 (1998).
[30] J. Joseph Sharkey, V. Dhanasekaran, ChangWoo Lee, A. John Peter, Chem. Phys. Lett. **503**, 86 (2011).
[31] M. A. Lampert, P. Mark, Current Injection in Solids, Academic Press, New York and London (1970).
[32] A.S. Aybek, M. Kul, E. Turan, M. Zor and E. Gedik, J. Phys.-Condens. Mat.**20**, 055216 (2008).
[33] Y. Lin, J. Zhang, E. H. Sargent, E. Kumacheva, Appl. Phys. Lett. **81**, Number 17 (2002).
[34] L. Spanhel, M. Haase, H.Weller, and A.Henglein, J. Am. Chem. Soc. **109**, 5649 (1987).
[35] M. Thambidurai, N. Muthukumarasamy, S. Agilan, N. Murugan, S. Vasantha, R. Balasundaraprabhu, T.S. Senthil, J Mater Sci. **45**, 3254 (2010).
[36] A.I. Olıva, J.E. Corona, R. Patıño and A.I. Olıva-Avılẽs, Bull. Mater. Sci. **37(**2), 247 (2014).
[37] M. Husham, Z. Hassan, A.M. Selman, N.K. Allam, Sensor Actuat. A-Phys. **230**, 9 (2015).